A Scalable Synthesis of (*R*,*R*)-*N*,*N*-Dibenzyl-2-fluorocyclohexan-1-amine with CsF under Hydrogen Bonding Phase-Transfer Catalysis

Anna Chiara Vicini,† Diké-Michel Alozie,‡[a] Philippe Courtes,‡[a] Giulia Roagna,† Catherine Aubert,‡[b] Victor Certal,‡[c] Youssef El-Ahmad,‡[c] Sébastien Roy,‡[b] Véronique Gouverneur†*

† University of Oxford, Chemistry Research Laboratory, 12 Mansfield Road, Oxford OX1 3TA, United Kingdom.

‡ Sanofi R&D, 13 Quai Jules Guesde, 94403 Vitry sur Seine Cedex, France. [a] Process Safety. [b] IDD Isotope Chemistry. [c] IDD Small Molecules Medicinal Chemistry.

KEYWORDS: β-Fluoroamines, Enantioselective Nucleophilic Fluorination, CsF, Phase-Transfer Catalysis, Hydrogen Bond Donor Catalyst

ABSTRACT: Hydrogen Bonding Phase-Transfer Catalysis (HB-PTC) offers a convenient solution to activate safe and economical metal alkali fluorides for enantioselective nucleophilic fluorination. Herein, we demonstrate the scalability of this protocol with the fluorination of 200 g of *rac*-(*R*,*R*)-*N*,*N*-dibenzyl-2-bromocyclohexan-1-amine in a mechanically stirred 1 L glass reactor using 0.5 mol% of bis-urea organocatalyst. In these experiments, full conversions were obtained for high mixing intensities (impeller average shear rate >10 000 s^{-1}; maximum energy dissipation per unit of mass >300 W/kg). The thermal safety of the reaction was assessed by differential scanning calorimetry (DCS) and reaction calorimetry (RC), assigning the reaction to Stoessel's critical class 3.

1. INTRODUCTION

Fluorine incorporation has a dramatic effect on the physical and chemical properties of organic molecules.[1] As such, it is a well-established strategy in the pharmaceutical and agrochemical industries to improve the properties of biologically active compounds.[2] As the number of fluorinated drugs on the market increases,[3] so does the demand for enantioselective protocols which employ safe, cheap and abundant fluorine sources.[4] The application of asymmetric phase-transfer catalysis (PTC) to industrial processes offers multiple advantages, such as the use of cheaper and safer raw materials, milder reaction conditions, and enhanced selectivity and yields.[5] Both cationic and anionic asymmetric PTC in combination with electrophilic fluorinating reagents have been reported,[6] but the high cost of these reagents is a disadvantage for large scale production. In contrast to electrophilic fluorination reagents derived from F_2, alkali metal fluorides are safe and inexpensive fluorine sources, which are available in bulk quantity from hydrogen fluoride.[7] Their use in asymmetric fluorination is challenging because of their poor solubility and the difficulties in balancing fluoride nucleophilicity and basicity.

We reported Hydrogen Bonding Phase-Transfer Catalysis (HB-PTC), a new concept in PTC that relies on the ability of a hydrogen bond donor to solubilize solid inorganic salts *via* complexation of the anion.[8–10] Control over enantioselectivity was achieved for nucleophilic fluorination with a new class of chiral BINAM-derived (BINAM = [1,1'-binapthalene]-2,2'-diamine) *N*-alkyl bis-urea catalysts capable of forming a tricoordinated hydrogen bonded fluoride complex **I** (Figure 1).[11] Pairing with a cationic electrophile leads to the chiral ion pair **II**, that undergoes fluorination with release of the enantioenriched fluorinated product and the catalyst. This metal-free organocatalyzed fluorination gave access to highly valuable enantioenriched β-fluoroamines (up to 92% yield and 96:4 e.r. = enantiomeric ratio) upon enantioselective desymmetrization of *meso* aziridinium ions generated *in situ* from stable precursors.[9] Both potassium fluoride (KF) and cesium fluoride (CsF) were suitable reagents for this protocol.

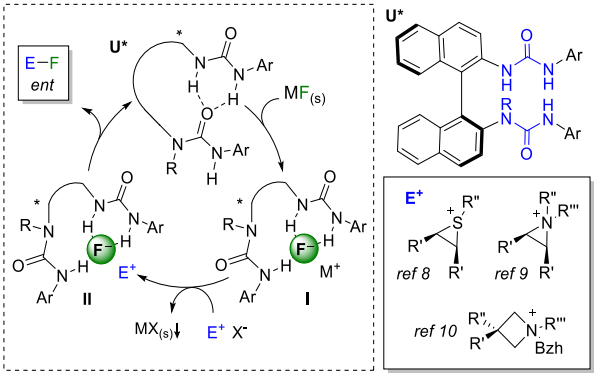

Figure 1: Asymmetric HB-PTC applied to metal alkali fluorides. Bzh= Benzhydryl. MF = CsF or KF; X = Cl, Br, OTf.

The mildness of enantioselective fluorination under HB-PTC, coupled with operational simplicity and the use of safe and economical fluoride sources,[12] prompted us to further investigate its scalability for initial assessment of its advantages and limitations from a process chemistry standpoint. As a model reaction, we focused on the 200 g-scale enantioselective fluorination of *rac*-(*R*,*R*)-*N*,*N*-dibenzyl-2-bromocyclohexan-1-amine *rac*-**1** (Figure 2A) in a mechanically stirred reactor. The multigram synthesis (>30 g) of the organocatalyst (*S*)-**3** used in this study has recently been achieved.[13]

Rac-**1** was selected as substrate because it gives access to enantiopure *trans*-2-fluorocyclohexan-1-amine, a highly valuable building block for discovery campaigns,[14–15] and represents a challenging substrate for enantioselective HB-PTC. Known high-yielding syntheses of a protected racemic precursor include the deoxyfluorination of *trans*-2-(dibenzylamino)cyclohexan-1-ol with explosive DAST (DAST = Diethylaminosulfur trifluoride) (70% yield),[16] and

the ring opening of the bicyclic tosyl aziridine with TBAF (69% yield).[14] Alternative approaches to racemic *trans*-2-fluorocyclohexan-1-amine or its protected analogues suffer from poor diastereoselectivity[17] or use hazardous reagents,[18] and are low-yielding.[17,18] In all cases, resolution with a chiral acid is required to afford the enantiopure compound, resulting in the waste of half of an expensive starting material. A protected precursor of *trans*-2-fluorocyclohexan-1-amine can be accessed in 92:8 e.r. using high loadings of two Lewis acids (Co-Salen: 5 mol% and $Ti(NMe_2)_4$: 10 mol%).[19] The protocol employs toxic and corrosive HF generated *in situ* from an excess of benzoyl fluoride and hexafluoroisopropanol (HFIP) and was not demonstrated on scale larger than 1 g.

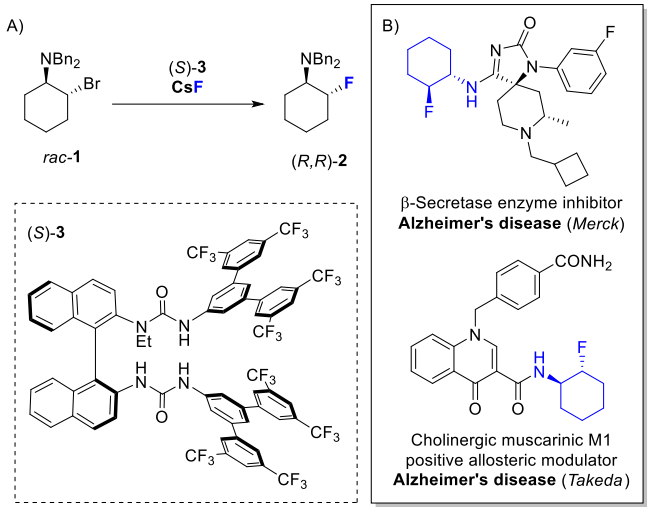

Figure 2: A) Model reaction for the scale-up of enantioselective nucleophilic fluorination under HB-PTC in a mechanically stirred 1 L reactor. B) Examples of bioactive compounds featuring the *trans*-2-fluorocyclohexan-1-amine motif.[14–15]

2. RESULTS AND DISCUSSION

We reported the fluorination of *rac*-**1** with KF (5 equiv) in the presence of 10 mol% of catalyst (*S*)-**3** in α,α,α-trifluorotoluene for 72 h; under these conditions (*R*,*R*)-**2** was isolated in 68% yield (78% ^{19}F NMR yield) and 85.5:14.5 e.r.[9] The reaction with CsF gave similar results (60% yield, 85:15 e.r.).

Optimization aimed at reducing catalyst loading revealed that solvent and concentration were important parameters (Tables 1 and S1−S3).[20] The reactivity of KF in the presence of 1 mol% of (*S*)-**3** was most favorable in $CHCl_3$, and afforded (*R*,*R*)-**2** in 59% yield after 72 h (Table 1, entry 2). The reaction with CsF was completed in 24 h when the same catalyst loading (1 mol%) was used (97% yield, 82:18 e.r., entry 4), and it was still efficient in the presence of 0.5 mol% of (*S*)-**3** (88% yield, 81:19 e.r., entry 5). Reducing the loading further to 0.2 mol% decreased both yield and e.r. (33% yield, 79:21 e.r., entry 6). A significative drop in yield was observed reducing the CsF equivalents from 3 (88%, entry 5) to 1.2 (42%, entry 15) in the presence of 0.5 mol% of (*S*)-**3**, but high yields could be restored doubling the concentration from 1 M to 2 M (87%, entry 16). For both fluoride salts, chlorinated solvents gave the best conversions (KF: entries 2−3; CsF entries 7−14). The reaction did not proceed or gave very low yields in $PhCH_3$ (21%, entry 9), BuCN (10%, entry 11),[21] 2-MeTHF (traces, entry 12), anisole (35%, entry 13) or EtOAc (traces, entry 14). Pleasingly, better results were secured in CH_2Cl_2 (90%, entry 7), $PhCF_3$ (65%, entry 8), and 1,2-DFB (1,2-difluorobenzene, 66%, entry 10). At lower catalyst loading (0.5 mol%) the yields obtained in $PhCF_3$ (12%, entry 17) and 1,2-DFB (30%, entry 18) were prohibitively low compared to the reaction performed in CH_2Cl_2 (87%, entry 16). For proof-of-scalability, further studies were therefore performed using 1.2 equiv of CsF, 0.5 mol% of (*S*)-**3**, in CH_2Cl_2 (2 M) (entry 16).

Table 1: Reaction Optimization[a]

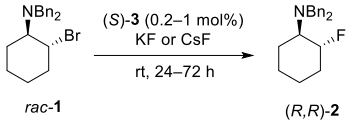

Entry	MF (equiv)	Solvent (Conc./M)	(*S*)-3 mol%	Yield[b]	e.r. [c]
1	KF (5)	$PhCF_3$ (2)	1	27%	84.5:15.5
2	KF (5)	$CHCl_3$ (2)	1	59%	81.5:18:5
3	KF (5)	CH_2Cl_2 (2)	1	45%	81.5:18.5
4	CsF (3)	CH_2Cl_2 (1)	1	97%	82:18
5	CsF (3)	CH_2Cl_2 (1)	0.5	88%	81:19
6	CsF (3)	CH_2Cl_2 (1)	0.2	33%	79:21
7	CsF (1.2)	CH_2Cl_2 (1)	1	90%	82:18
8	CsF (1.2)	$PhCF_3$ (1)	1	65%	85:15
9	CsF (1.2)	$PhCH_3$ (1)	1	21%	-
10	CsF (1.2)	1,2-DFB (1)	1	66%	81.5:18.5
11	CsF (1.2)	BuCN (1)	1	10%	-
12	CsF (1.2)	2-MeTHF (1)	1	traces	-
13	CsF (1.2)	Anisole (1)	1	35%	84:16
14	CsF (1.2)	EtOAc (1)	1	traces	-
15	CsF (1.2)	CH_2Cl_2 (1)	0.5	42%	81.5:18.5
16	**CsF (1.2)**	CH_2Cl_2 **(2)**	**0.5**	**87%**	**82:18**
17	CsF (1.2)	$PhCF_3$ (2)	0.5	12%	85:15
18	CsF (1.2)	1,2-DFB (2)	0.5	30%	82:18

[a] Reaction conditions: *rac*-**1** (90 mg, 0.25 mmol), KF or CsF and (*S*)-**3** were weighed in a vial followed by addition of the solvent. The reaction was stirred at rt, at 900 rpm for 72 h (KF) or 24 h (CsF). [b] Yield determined by ^{19}F NMR using 4-fluoroanisole as internal standard. [c] e.r. determined by HPLC on a chiral non-racemic stationary phase. 1,2-DFB = 1,2-difluorobenzene.

Next, we evaluated the effect of CsF granulometry and purity, as well as water content on the reaction outcome (Table 2). As expected, particle size played a major role for efficient phase transfer (entries 1−2). The reaction was not influenced by CsF purity (entries 2−3), while the water content impacted on reactivity but not on enantioselectivity (entries 3−6). "Wet" CsF as provided from the supplier[22] performed better than dried CsF[23] (86% *versus* 74% yield, entries 3−4). Deliberate addition of 10 mol% and 50 mol% of water (0.46% and 4.8% mass of H_2O/mass CsF) decreased the yield to 65% and <5%, respectively (entries 5−6). Both CsF granulometry and water content are thus important parameters to ensure reaction reproducibility. For this reason, we suggest storing CsF in a desiccator for laboratory use.

Table 2: Effect of CsF Purity, Granulometry, and Water Content[a]

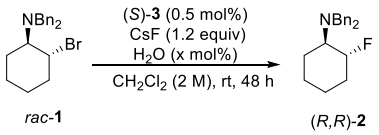

Entry	CsF (purity)	H_2O/ CsF (w/w %)	Yield [b]	e.r. [c]
1	Particle[d] (99.9%)	–	25%	81.5:18.5
2	Powder[e] (99.9%)	–	87%	81.5:18.5
3	Powder[e], [f] (99%)	–	86%	81:19
4	Powder[e], dry[g] (99%)	–	74%	81.5:18.5
5	Powder[e], dry[g] (99%)	H_2O (0.96)	65%	82:18
6	Powder[e], dry[g] (99%)	H_2O (4.8)	< 5%	–

[a] Reaction conditions: *rac*-**1** (500 mg, 1.40 mmol), CsF (260 mg, 1.2 equiv) and (*S*)-**3** (9.8 mg, 0.5 mol%) were weighed in a vial, followed by addition of CH_2Cl_2 (700 µL, 2 M) and H_2O, if any. The reaction was stirred at rt, at 900 rpm for 24 h. [b] Yield determined by ^{19}F NMR using 4-fluoroanisole as internal standard. [c] e.r. determined by HPLC on a chiral non-racemic stationary phase. [d] Particle distribution: 1–2 mm. [e] Particle distribution: 2–300 µm. [f] Water content: 0.98% w/w. [g] CsF was dried *in vacuo* at 200 °C for 48 h. Reaction performed using Schlenk techniques.

In preparation of the scale-up, we examined the effect of the order of addition of the reagents on a 0.5 g scale of *rac*-**1** (Table 3, entries 1–3). Mixing all the solid reagents followed by addition of CH_2Cl_2 (batch conditions) afforded (*R*,*R*)-**2** in 88% yield and 81.5:18.5 e.r. after 24 h (entry 1). A similar result was obtained pre-stirring CsF and (*S*)-**3** in CH_2Cl_2 for 45 min, followed by the addition of *rac*-**1** as a solid (83% yield in 24 h, 82:18 e.r., entry 2). Inverting the addition order by adding solid CsF to a stirred solution of *rac*-**1** and (*S*)-**3** in CH_2Cl_2 did not change the reaction outcome (82% yield in 24 h, 82:18 e.r., entry 3). The scalability of the reaction in magnetically stirred round-bottom flasks (RBFs) was evaluated on a scale from 5 to 50 g (entries 4–7). Reproducibility of the fluorination was assessed running two parallel reactions on 5 g of *rac*-**1** employing reagents and catalyst (*S*)-**3** from different suppliers and batches (entries 4–5). Comparable conversions and e.r. were obtained, prompting us to further scale up the fluorination to 10 g (entry 6) and 50 g (entry 7). In all cases the reaction was complete within 48 h and the only product obtained was β-fluoroamine (*R*,*R*)-**2** in 81.5:18.5 e.r..

Table 3: Scale-up in Magnetically Stirred Vessels[a]

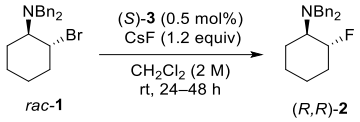

Entry	Scale	Time	Yield [b]	e.r. [c]
1	0.5 g (batch)	24 h	88%	81.5:18.5
2[d]	0.5 g (semi-batch)	24 h	83%	82:18
3[e]	0.5 g (semi-batch)	24 h	82%	82:18
4 [f]	5 g (batch)	48 h	>99%	81.5:18.5
5 [g]	5 g (batch)	48 h	>99%	81:19
6	10 g (batch)	48 h	98%	82:18
7	50 g (batch)	48 h	98% (90%)	81.5:18.5

[a] Reaction conditions: *rac*-**1**, CsF (1.2 equiv) and (*S*)-**3** (0.5 mol%), were stirred in CH_2Cl_2 (2 M) at rt and 900 rpm in a vial or RBF for 24–48 h. [b] Yield determined by ^{19}F NMR using 4-fluoroanisole as internal standard; yield of isolated product in parenthesis. [c] e.r. determined by HPLC on a chiral non-racemic stationary phase. [d] (*S*)-**3** and CsF were stirred in CH_2Cl_2 for 45 min before addition of *rac*-**1** as a solid. [e] (*S*)-**3** and *rac*-**1** were stirred in CH_2Cl_2 for 45 min before addition of solid CsF. [f] *rac*-**1** synthetized in Oxford; CsF from Sigma-Aldrich (99%); (*S*)-**3**: from a batch different to the one used in the scale-up; CH_2Cl_2 from Sigma-Aldrich (stabilized with amylene). [g] *rac*-**1** from WuXi AppTec; CsF from Fluorochem (99%), (*S*)-**3** from the same batch used in the scale-up, CH_2Cl_2 from Carlo Erba Reagents (stabilized with amylene).

To evaluate the performance of the fluorination in a mechanically stirred vessel, we performed the reaction on 200 g of *rac*-**1** in a 1 L jacketed laboratory reactor (OptiMax) equipped with a 45° down-pumping four-bladed PBT (pitched blade turbine), a flat glass baffle, a calibration probe, and a temperature probe (Figures 3A and 3B). The reactor was charged with *rac*-**1** (200 g) and CH_2Cl_2 (280 ml). When the substrate was solubilized (judged visually), the catalyst (*S*)-**3** (3.9 g, 0.5 mol%) was added, followed by solid CsF (104 g) in a single charge. ^{19}F NMR analysis revealed that 75% of the product was formed within 22 h and 97% yield was achieved in 46 h. This result compares favorably with a 10 g reaction performed in a magnetically stirred RBF (88% and 99% yield after 21 h and 48 h, respectively; Figure 3C). At the end of the reaction, the product was separated from the catalyst by acid-base extraction (HCl/NaOH), which afforded 157.39 g of (*R*,*R*)-**2** (95% yield, 81.5:18.5 e.r.). The amine was neutralized with trifluoroacetic acid and the resulting salt was recrystallized from ^{i}PrOH (1 mL/g) to afford 115.7 g of (*R*,*R*)-**2**•CF_3COOH in 98:2 e.r. (53%).

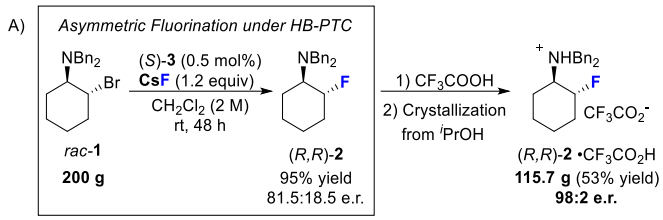

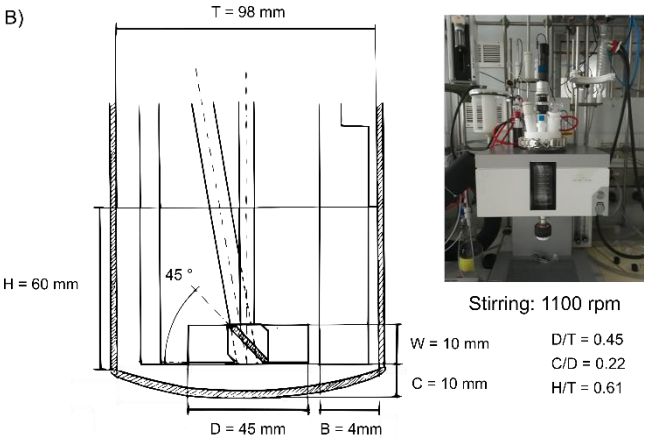

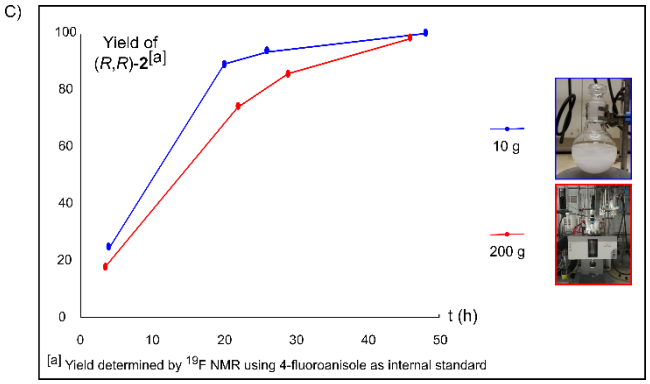

Figure 3: A) Scale-up of enantioselective fluorination under HB-PTC in a mechanically stirred reactor; B) reactor set-up; C) comparison of the fluorination in a RBF (10 g, blue) and in the OptiMax (200 g, red).

To collect further data, we repeated the reaction on 200 g of *rac*-**1** in a 1 L Radleys reactor, equipped with a PTFE 45° down-pumping four-bladed PBT and 4 flat baffles located 90° apart. The maximum motor speed for this set-up was 678 rpm compared to the 1100 rpm reached by the OptiMax motor. After 24 h, the yield of (*R*,*R*)-**2** was 11% and did not improve in the following 48 h. Samples were taken at 24 h and 48 h, and transferred in vials equipped with a magnetic stirring bar. No catalyst nor CsF were added to these samples. Stirring these aliquots for further 48 h afforded (*R*,*R*)-**2** in 58% and 77% yield, respectively. These results suggest that the low conversion in the Radleys reactor was due to poor mixing. Both CsF and CsBr are dense solids (4.12 g/cm^3 and 4.44 g/cm^3 respectively), and the mechanical stirrer serves the purpose to suspend these inorganic salts. From visual inspection, this was achieved in both reactors. The energy dissipation of the reactor set-up may influence conversion. In a preliminary analysis, Dynochem was used to assess mixing parameters at this scale (≤1 L).[24] We compared the local maximum energy dissipation rate in the impeller region (ε_{max})[25] and the impeller averaged turbulent shear rate (γ_{imp})[26] of four trials characterized by different reactor set-ups and conversions (Table 4). A significative difference in the value of these parameters was found between the reactions that stalled below 50% conversion (entries 3–4) and those that reached completion within the same period (entries 1–2). Full conversions were obtained above a threshold of 300 W/kg for the local maximum energy dissipation rate ε_{max} and of 10 000 s^{-1} for the impeller average shear rate γ_{imp}.

Table 4: Hydrodynamic Parameters[a]

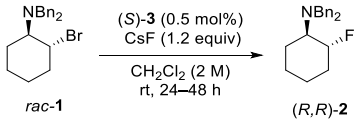

Entry	Reactor Volume	Conversion[b] (48 h)	ε_{max} (W/Kg)	γ_{imp} (s^{-1})
1	22 mL	95%	330	12 000
2	1 L	97%	310	10 000
3	1 L	11%	80	5 000
4	0.5 L	56%	20	2 000

[a] Conditions: *Entry 1:* TOP45 autoclave reactor (tank: 725-4), 22 cm^3, 100% baffled, four-bladed turbine, 2050 rpm, 3 g of *rac*-**1**. *Entry 2:* OptiMax HFCal Mettler Toledo, 1 L, 98% baffled, 45° down-pumping four-bladed PBT, 1100 rpm, 200 g of *rac*-**1**. *Entry 3:* Radleys reactor, 1 L, 100% baffled, 45° down-pumping four-bladed PBT, 678 rpm, on 200 g of *rac*-**1**. *Entry 4:* RC1AP01 calorimeter Mettler Toledo, 0.5 L, 31% baffled (temperature and calibration probes), 45° down-pumping four-bladed PBT, 600 rpm, 100 g of *rac*-**1**; [b] Determined by ^{1}H NMR using 4-fluoroanisole as internal standard.

Intense mixing could result in smaller CsBr particle size distribution, leading to increased wall deposit and possibly negatively impacting the filterability of the crude reaction mixture.[27] Samples of CsBr formed in this 200 g scale reaction were analyzed by optical and scanning electron microscopy (SEM) revealing agglomerates (~100 µm) of spherical particles of 5–10 µm (Figure 4).

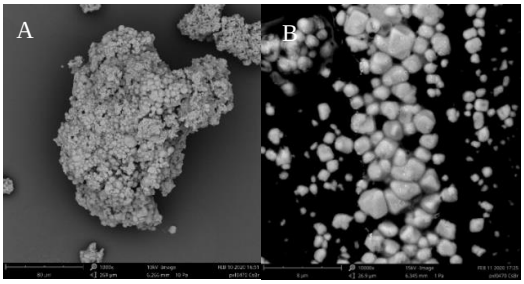

Figure 4: SEM analysis of a sample of CsBr obtained upon fluorination on 200 g of *rac*-**1**. Coating: gold, 120 s; Voltage: 10 kV–15 kV; A) x 1 000; B) x 10 000.

The thermal safety of the fluorination under HB-PTC was examined next. Differential scanning calorimetry (DSC) tests were performed on pure (*S*)-**3**, *rac*-**1** and (*R*,*R*)-**2**, as well as on the initial (sampled immediately after CsF addition) and final (sampled after 48 h) reaction mixtures. No major decomposition (> 100 J/g) was observed below 150 °C during a standard dynamic test (scanning rate 5 °C/min, static air atmosphere, high pressure sealed gold-plated crucible). The initial and final reaction mixtures mirrored the curves of the starting material and product, respectively, but the energy released during their decomposition was substantially reduced due to the dilution effect of CH_2Cl_2 (initial reaction mixture: 40 J/g, *versus* pure *rac*-**1**: 159 J/g; final reaction mixture: two peaks of 41 J/g and 74 J/g, *versus* pure (*R*,*R*)-**2**: 274 J/g).[28] The 200 g scale fluorination was performed in a Mettler Toledo OptiMax heat flow calorimeter (HTCal).[28] Solubilization of *rac*-**1** in CH_2Cl_2 is an endothermic process (ΔH = +28 kJ/mol) which results in an adiabatic temperature drop (ΔT_{ad}) of 22 °C, while catalyst addition only marginally perturbates the heat flow. Product formation following CsF charge is exothermic (ΔH = –30 kJ/mol of *rac*-**1** or q_R = 24.7 kJ/kg of reaction mass) and presents high thermal accumulation (95%) at the end of CsF addition. This corresponds to ΔT_{ad} = +28 °C. The maximum temperature of the synthesis reaction (MTSR), which is the maximum temperature reached by the reaction mass in adiabatic conditions—e.g. in case of cooling failure—would be 50 °C ($T_p + \Delta T_{ad}$ = 22 °C + 28 °C, Table 5). This exceeds the boiling point of the solvent (CH_2Cl_2, Bp: 39.6 °C, Table 5), but it is more than 100 °C below the onset of thermal decomposition of both the initial and final reaction mixtures (170 °C and 245 °C respectively) as determined by DSC analysis. These data permit to assign the fluorination to the critical class 3, according to Stoessel's classification.[29] Since solvent evaporation constitutes a safety barrier to the loss of control of the main reaction, the use of a condenser of appropriate size is required to minimize the thermal risk. This is also mitigated by the fact that the reaction is slow (48 h), and no gas is generated in the process.

Table 5: Process Parameters for Critical Class Definition

Parameter	Value	Comment
T_p	22 °C	Process Temperature
MTT	40 °C	CH_2Cl_2 Bp
ΔT_{ad}	28 °C	From RC
MTSR	50 °C	From RC
T_{onset}	170 °C	From DSC on the initial reaction mixture
T_{exo}	70 °C	T_{onset} −100 °C

MTT= Maximum Technical Temperature; in an open system, this corresponds to the solvent boiling point. MTSR = Maximum Temperature of the Synthesis Reaction; the maximum temperature reached by the reaction mass in adiabatic conditions due to the heat released by the main reaction. RC = Reaction Calorimetry. DSC = Differential Scanning Calorimetry.

3. CONCLUSIONS

HB-PTC was successfully applied to the scale-up of the enantioselective fluorination of 200 g of racemic *trans*-*N*,*N*-dibenzyl-2-bromocyclohexan-1-amine *rac*-**1** in the presence of *N*-alkyl bis-urea (*S*)-**3**. The reaction afforded β-fluoroamine (*R*,*R*)-**2** in excellent yield (95%, 157.39 g) and no erosion of enantioselectivity compared to the smaller scale reactions (81.5:18.5 e.r.). The enantiomeric ratio was enhanced (98:2 e.r.) by single recrystallization of the CF_3COOH salt of (*R*,*R*)-**2** from ^{i}PrOH (115.7 g). The fluorination protocol is characterized by an easy set-up and, for reactions using up to 50 g of *rac*-**1**, can be carried out in standard laboratory glassware without pre-treatment of CsF (fine powder). CsF particle size distribution and water content are important parameters to ensure reproducibility. Scale-up (200 g) in a 1 L mechanically stirred reactor has been demonstrated. The use of an axial impeller and baffles is recommended to ensure optimal suspension of solid CsF. Under these conditions, the best conversions were obtained when the local energy dissipation rate ε_{max} and the local turbulent shear rates γ_{imp} were superior to 300 W/kg and 10000 s^{-1}, respectively. The thermal safety of the reaction was evaluated by DSC and RC which allowed to categorize this fluorination protocol into Stoessel's critical class 3.

4. EXPERIMENTAL SECTION

4.1. General experimental The synthesis of starting material *rac*-**1** was outsourced to WuXi AppTec according to literature procedure[9] and the substrate was used as provided. The multigram synthesis of catalyst (*S*)-**3** is reported elsewhere.[13] KF (99.9% trace metal basis from Alfa Aesar) was used as provided by the supplier (fine powder) and used without pre-drying. CsF (Fluorochem, 99% purity, water content 0.98% w/w determined by Karl-Fisher titration) was used as provided by the supplier (fine powder, particle distribution 2−300 μm) and used without pre-drying. The same batch was used during the whole scale-up. CH_2Cl_2 was purchased either from Sigma-Aldrich (≥ 99.8%, for HPLC, stabilizer: amylene) or Carlo Erba Reagents (≥ 99.98%, stabilizer: amylene). All NMR spectra were recorded on Bruker AVANCE III HD 400 or AVANCE NEO 400. ^{1}H and ^{13}C NMR spectral data are reported as chemical shifts (δ) in parts per million (ppm) relative to the solvent peak using the Bruker internal referencing procedure (edlock). ^{19}F NMR spectra are referenced relative to Trifluoroacetic acid (TFA). Data are reported as follows: chemical shift, multiplicity (s = singlet, d = doublet, t = triplet, q = quartet, pent = pentet, sept = septet, br = broad, m = multiplet), coupling constants (Hz) and integration. The Fluorination was monitored by ^{1}H and ^{19}F NMR using 4-fluoroanisole as internal standard. The enantiomeric ratios were determined by HPLC analysis on a Shimadzu *i*-Prominence LC-2030 (PDA detector) employing a DAICEL CHIRALPAK® IB-3 by comparing the samples with the racemic mixture.

4.2. Enantioselective Fluorination under HB-PTC

Reaction: A OptiMax HFCal Mettler Toledo 1 L glass reactor (diameter 98 mm, dish bottom head) equipped with a 45 mm glass 45 °down-pumping four-bladed PBT (pitched blade turbine), a 4 mm glass baffle, a temperature probe and a calibration probe (see Figure 3B) was charged with 250 mL of CH_2Cl_2 followed by solid *rac*-**1** (200 g, 0.558 mol). The temperature of the jacket was set at 22 °C and the stirring speed at 1100 rpm. Full solubilization (judged visually, ~10 min) and temperature stabilization at 22 °C was achieved prior to performing the first calibration. The stirring speed was reduced to 300 rpm and solid catalyst (*S*)-**3** (3.9 g, 0.5 mol%) was added followed by further 30 mL of CH_2Cl_2 (to wash the flask and funnel). Full solubilization (judged visually, ~ 30 s) was achieved prior to the addition of solid CsF (104 g, 1.2 equiv) as a single charge. The stirring rate was increased to 1100 rpm and the reaction stirred at this speed until full conversion (monitored by ^{1}H and ^{19}F NMR) which was reached after 48 h. A second calibration was performed at this point. **Reaction monitoring (NMR):** Samples were taken from the stirred reactor and filtered using a 13 mm syringe filter (0.45 μm PTFE). Exactly 50 μL of filtrate were transferred in a vial and evaporated to dryness. 10 μL of 4-fluoroanisole and 1 mL of $CDCl_3$ were added and both ^{1}H NMR (to estimate the conversion) and quantitative ^{19}F NMR (to obtain the yield) were recorded. **Work-up:** The reactor was emptied and washed with 600 mL of CH_2Cl_2: ^{i}Pr$_2$O = 1:1 (2x 300 mL each wash). The combined organic phases were filtered on a plug of Clarcel® filter aid (4 cm high), eluting with further 100 mL of CH_2Cl_2: ^{i}Pr$_2$O = 1:1. The filtrate was evaporated *in vacuo* to obtain 160 g of crude **2**. The crude product was dissolved in ^{i}Pr$_2$O (800 mL) and extracted with $HCl_{(aq)}$ 1 M (3x 500 mL). The aqueous phase was neutralized with $NaOH_{(aq)}$ 5 M (300 mL, pH = 8, monitored by pH-paper) and extracted with CH_2Cl_2 (800 mL followed by 2x500 mL). The combined organic layers were washed with brine (500 mL), passed through a $MgSO_4$ pad and evaporated *in vacuo* to afford (*R*,*R*)-**2** as a white solid (157.39 g, 95% yield, 81.5:18.5 e.r.). **Purification:** The product was fully solubilized in ^{i}PrOH (500 mL) at 60 °C and trifluoroacetic acid (40.5 mL, 1 equiv) was added dropwise while stirring to form the corresponding salt. Volatiles were removed *in vacuo* to afford a white powdery solid (217.7 g) which was dissolved in refluxing ^{i}PrOH (218 mL). Crystallization was achieved by slowly (over 2 h) cooling the solution to 35 °C, temperature that was maintained for further 4 h. (*Note:* control of the crystallization time is necessary to achieve a good level of enantioenrichment). After this time, the solid was filtered and washed twice with cold (+4 °C) ^{i}PrOH to afford 115.7 g of CF_3COOH•(*R*,*R*)-**2** in 98:2 e.r. (115.7 g, 53% recrystallization yield). **Characterization:** *Spectroscopic data of the free base* (*R*,*R*)-**2** were in agreement with the ones previously reported in the literature.[9] **$[\alpha]_D^{25\,°C}$ =** – 18.4° (c 0.8, $CHCl_3$, e.r. = 98:2). *Spectroscopic data of the trifluoroacetic salt* CF_3COOH•(*R*,*R*)-**2***:* **^{1}H NMR** (500 MHz, $CDCl_3$) δ 11.93 (br s, 1H), 7.55 (dd, *J* = 7.4, 2.2 Hz, 4H), 7.41 – 7.33 (m, 6H), 4.86 (dtd, *J* = 51.3, 10.5, 4.8 Hz, 1H), 4.40 (d, *J* = 13.1 Hz, 2H), 4.24 (d, *J* = 13.1 Hz, 2H), 3.26 (dtt, *J* = 13.7, 10.4, 4.7 Hz, 1H), 2.34 – 2.14 (m, 2H), 1.75 – 1.55 (m, 2H), 1.38 (tddd, *J* = 12.6, 10.7, 8.4, 4.1 Hz, 1H), 1.24 (qd, *J* = 12.7, 3.7 Hz, 1H), 1.18 – 0.93 (m, 2H); **^{19}F NMR** (471 MHz, $CDCl_3$) δ −75.64 (3F), −174.40 (d, *J* = 52.6 Hz, 1F);

^{13}C NMR (126 MHz, $CDCl_3$) δ 161.6 (q, *J* = 35.4 Hz), 131.9 (br), 131.0, 129.4, 129.1, 116.8 (q, *J* = 292.5 Hz), 91.4 (d, *J* = 178.9 Hz), 63.4 (d, *J* = 14.2 Hz), 56.8 (br), 32.4 (d, *J* = 17.3 Hz), 27.4 (d, *J* = 6.6 Hz), 24.5 (d, *J* = 2.1 Hz), 23.3 (d, *J* = 11.2 Hz); **MP:** 103–105 °C; **$[\alpha]_D^{25\,°C}$ =** –2.8 ° (c 1.2, $CHCl_3$, e.r. = 98:2). All the e.r. were determined on the free base. The e.r. of recrystallized CF_3COOH•(*R*,*R*)-**2** was determined on 5 samples taken randomly and neutralized with $NaOH_{(aq)}$ 5 M, extracted with heptane and analyzed by chiral HPLC. HPLC separation: DAICEL CHIRALPAK® IB-3, Heptane:^{i}PrOH = 99.5:0.5, 1 mL/min; t_1 = 3.46 min (minor), t_2 = 4.49 min (major).

ASSOCIATED CONTENT

Additional optimization data; CsF and CsBr particle size distribution analysis; Dynochem calculations; DSC curves; RC data; catalyst recycling; copy of ^{1}H ^{19}F and ^{13}C NMR spectra; copy of HPLC traces.

AUTHOR INFORMATION

Corresponding Author

veronique.gouverneur@chem.ox.ac.uk

Notes

The authors declare no competing financial interests.

ACKNOWLEDGMENT

We acknowledge Dr. Serge Perard for his assistance in NMR analysis, Patrick Richepin for his technical assistance, Dr. Benoit Robert for analysis of CsF and CsBr particles by SEM and optical microscopy, and Ing. Philippe Perrichon, Christian Poma, Dr. Francesco Ibba for useful discussions. This work was supported by the EU Horizon 2020 Research and Innovation Program (Marie Skłodowska-Curie agreements 675071).

ABBREVIATIONS and SYMBOLS

BINAM: [1,1'-binapthalene]-2,2'-diamine
Bzh: Benzhydryl
1,2-DFB = 1,2-difluorobenzene
DSC: Differential Scanning Calorimetry
e.r.: enantiomeric ration
FCC: Flash Column Chromatography
HB-PTC: Hydrogen Bonding Phase-Transfer Catalysis
MTSR: Maximum Temperature of the Synthesis Reaction
MTT= Maximum Technical Temperature
PBT= Pitched Blade Turbine
RC: Reaction Calorimetry
SEM: Scanning Electron Microscopy

D = Impeller diameter (m)
ε_{max} = Local maximum energy dissipation rate in the impeller region (W/kg)
γ_{imp} = Impeller shear rates (s^{-1})
N = Impeller speed (s^{-1})
μ = Liquid viscosity (Pa*s)
P= Power input (W)
P_0 = Power number

REFERENCES

1) (a) Müller, K.; Faeh, C.; Diederich, F. Fluorine in Pharmaceuticals: Looking Beyond Intuition. *Science* **2007**, *317*, 1881–1886. (b) Purser, S.; Moore, P. R.; Swallow, S.; Gouverneur, V. Fluorine in Medicinal Chemistry. *Chem. Soc. Rev.* **2008**, *37*, 320–330. (c) Gillis, E. P.; Eastman, K. J.; Hill, M. D.; Donnelly, D. J.; Meanwell, N. A. Applications of Fluorine in Medicinal Chemistry. *J. Med. Chem.* **2015**, *58*, 8315–8359.

2) (a) *Fluorine in Medicinal Chemistry and Chemical Biology*, Ojima, I., Ed.; Wiley-Blackwell: Chichester, UK, 2009. (b) *Fluorine in Pharmaceutical and Medicinal Chemistry*, Gouverneur, V., Müller, K., Eds.; Imperial College Press: London, UK, 2012. (c) Jeschke, P. The Unique Role of Fluorine in the Design of Active Ingredients for Modern Crop Protection. *ChemBioChem* **2004**, *5*, 570–589.

3) Inoue, M.; Sumii, Y.; Shibata, N. Contribution of Organofluorine Compounds to Pharmaceuticals *ACS Omega* **2020**, *5*, 10633–10640.

4) (a) Bryan, M. C.; Dunn, P. J.; Entwistle, D.; Gallou, F.; Koenig, S. G. ; Hayler, J. D.; Hickey, M. R.; Hughes,S.; Kopach, M. E.; Moine, G.; Richardson, P.; Roschangar, F.; Steven, A.; Weiberth, F. J. Key Green Chemistry Research Areas from a Pharmaceutical Manufacturers' Perspective Revisited *Green Chem.* **2018**, *20*, 5082–5103; (b) Caron, S. Where Does the Fluorine Come From? A Review on the Challenges Associated with the Synthesis of Organofluorine Compounds *Org. Process Res. Dev.* **2020**, *24*, 4, 470–480.

5) (a) Shirakawa, S.; Maruoka, K. Recent Developments in Asymmetric Phase-transfer Reactions. *Angew. Chem. Int. Ed.* **2013**, *52*, 4312–4348; (b) Burke, A. J., Marques, C. S., Turner, N. J., Hermann, G. J. Phase Transfer Catalysis. In *Active Pharmaceutical Ingredients in Synthesis: Catalytic Processes in Research and Development*, Wiley-VCH Verlag GmbH & Co. KGaA: Weinheim, Germany, 2018; pp 359–386.

6) For selected examples using cationic salts, see: (a) Wang, X.; Lan, Q.; Shirakawa, S.; Maruoka, K. Chiral Bifunctional Phase Transfer Catalysts for Asymmetric Fluorination of β-Keto Esters *Chem. Commun*. **2010**, *46*, 321–323; (b) Kim, D. Y.; Park, E. J. Catalytic Enantioselective Fluorination of β-Keto Esters by Phase-Transfer Catalysis Using Chiral Quaternary Ammonium Salts *Org. Lett.* **2002**, *4*, 545–547; for anionic salts, see: (b) Rauniyar, V.; Lackner, A. D.; Hamilton, G. L.; Toste, F. D. Asymmetric Electrophilic Fluorination Using an Anionic Chiral Phase-Transfer Catalyst *Science* **2011**, *334*, 1681–1684 (c) Yang, X.; Phipps, R. J; Toste, F. D. Asymmetric Fluorination of α-Branched Cyclohexanones Enabled by a Combination of Chiral Anion Phase-Transfer Catalysis and Enamine Catalysis using Protected Amino Acids *J. Am. Chem. Soc.* **2014**, *136*, 5225–5228.

7) Harsanyi, A; Sandford, G. Organofluorine Chemistry: Applications, Sources and Sustainability *Green Chem.* **2015**, *17*, 2081–2086.

8) Pupo, G.; Ibba, F.; Ascough, D. M. H.; Vicini, A. C.; Ricci, P.; Christensen, K. E.; Pfeifer, L.; Morphy, J. R.; Brown, J. M.; Paton, R. S.; Gouverneur, V. Asymmetric Nucleophilic Fluorination under Hydrogen Bonding Phase-Transfer Catalysis *Science*, **2018**, *360*, 638–642.

9) Pupo, G.; Vicini, A. C.; Ascough, D. M. H.; Ibba, F.; Christensen, K. E.; Thompson, A. L.; Brown, J. M.; Paton, R. S.; Gouverneur, V. Hydrogen Bonding Phase-Transfer Catalysis with Potassium Fluoride: Enantioselective Synthesis of β-Fluoroamines *J. Am. Chem. Soc.*, **2019**, *141*, 2878–2883.

10) Roagna, G.; Ascough, D. M. H.; Ibba, F.; Vicini, A. C.; Fontana, A.; Christensen, K. E.; Peschiulli, A.; Oehlrich, D.; Misale, M.; Trabanco, A.; Paton, R. S.; Pupo, G.; Gouverneur, V. Hydrogen Bonding Phase-Transfer Catalysis with Ionic Reactants: Enantioselective Synthesis of γ-Fluoroamines *J. Am. Chem. Soc.* **2020**, *142*, 14045–14051.

11) Ibba F.; Pupo, G.; Thompson, A. L.; Brown, J. M.; Claridge, T. D. W.; Gouverneur, V. Impact of Multiple Hydrogen Bonds with Fluoride on Catalysis: Insight from NMR Spectroscopy. *J. Am. Chem. Soc.* **2020**, 142, 19731–19744.

12) Bulk prices (100 Kg) of KF: 29.48 $/Kg (1.77 $/mol), CsF: 117.91 $/Kg (17.7 $/mol), and TBAF (1 M in THF): 70.75 $/Kg of solution (76.64 $/mol). October 2019.

13) Vicini, A. C., Pupo, G., Ibba, F., Gouverneur, V. Multigram Synthesis of *N*-Alkyl *Bis*-Ureas for Asymmetric Hydrogen Bonding Phase-Transfer Catalysis **2021** *Unpublished data (manuscript under revision).*

14) Coburn, C. A.; Egbertson, M. S.; Graham, S. L.; McGaughey, G. B.; Stauffer, S. R.; Yang, W.; Lu, W.; Fahr, B. Preparation of Triazaspirodecenones as β-Secretase Inhibitors for the Treatment of Alzheimer's Disease. Patent WO2007011833, 2007.

15) Sakamoto H., Sugimoto T. Preparation of Heterocyclic Compounds as Cholinergic Muscarinic M1 Receptor Positive Allosteric Modulators. Patent WO2013129622, 2013.

16) Chong, H.-S.; Sun X.; Chen Y.; Wang M. Synthesis, Characterization, and Nucleophilic Ring Opening Reactions of Cyclohexyl-Substituted β-Haloamines and Aziridinium Ions *Tetrahedron Letters*, **2015**, *56*, 946–948.

17) Eriksen, B. L.; Gustafsson, M.; Hougaard, C.; Jacobsen, T. A.; Jefson, M. R.; Klein, J.; Larsen, J. S; Lowe, J. A. III; McCall, J. M.; Stroøebæk, D.; Von Schoubye, N. L.; Keaney, G. F. Preparation of Cycloalkylamino Nitrogen Heterocycles as Potassium Channel Modulators for the Treatment and Prevention of Disorders. Patent WO2017210545, 2017.

18) (a) Wade, T. N. Preparation of Fluro Amines by Reaction of Aziridines with Hydrogen Fluoride in Pyridine Solution. *J. Org. Chem.* **1980**, *45*, 5328–5333; (b)Alvernhe, G.M.; Ennakoua, C. M.; Lacombe, S. M., Laurent, A. J. Ring Opening of Aziridines by Different Fluorinating Reagents: Three Synthetic Routes to α,β-Fluoro Amines with Different Stereochemical Pathways. *J. Org. Chem*, **1981**, *46*, 4938–4948.

19) Kalow, J., Doyle, A. Enantioselective Fluoride Ring Opening of Aziridines Enabled by Cooperative Lewis Acid Catalysis *Tetrahedron*, **2013**, *69*, 5702–5709

20) These screening reactions were conducted in batch, with the solvent added last to a glass vial containing the solid reagents.

21) *Rac*-**1** is not soluble in CH_3CN.

22) Water content 0.98% w/w H_2O/CsF, determined by Karl-Fisher titration.

23) Dried *in vacuo* at 200 °C for 48 h. Reaction performed using Schlenk techniques.

24) Dynochem 5, Scale-up Systems Limited, Dublin, Ireland (2019) www.scale-up.com (accessed May 11, 2020), based on the following references: (a) Metzner, A. B.; Otto, R. E. Agitation of non-Newtonian fluids, *AIChE J.* **1957**, *3*, 3–10; (b) Sánchez Pérez, J. A.; Rodríguez Porcel, E. M.; Casas López, J. L.; Fernández Sevilla, J. M.; Chisti, Y. Shear Rate in Stirred Tank and Bubble Column Bioreactors. *Chem. Eng. J.* **2006**, *124*, 1–5. (c) Mishra, V. P.; Joshi, J. B. LDA Measurements of Flow in Stirred Gas-Liquid Reactors, Fluid Mechanics of Mixing. In *Fluid mechanics of mixing. Fluid mechanics and its applications*; King, R., Ed.; Springer: Dordrecht, the Netherlands, 1992; pp 217–224; (d) Grenville, R. K.; Brown, D. A. R. A Method for Comparing Impellers' Generation of Flow and Turbulence. In *MIXING XXIII*; Mayan Riviera, Mexico, 2012.

25) $\varepsilon_{max} = 0.104\chi P_o^{¾} N^3D^2$, where χ=15

26) $\gamma_{imp} = (0.3P/(V_{imp}*\mu))^{1/2}$, where V_{imp} is the bottom impeller zone volume calculated according to $V_{imp} = D^2/(4\pi*D/4)$.

27) Further investigations on the effect of mixing is suggested prior to scale-up to vessels >1 L.

28) For further details, see the SI.

29) Stoessel, F. *Thermal Safety of Chemical Processes*; Wiley-VCH Verlag GmbH & Co. KGaA: Weinheim, Germany, 2008.

TABLE OF CONTENT